ANTIOXIDANTS & REDOX SIGNALING
Volume 14, Number 6, 2011

DOI: 10.1089/ars.2010.3587

ORIGINAL RESEARCH COMMUNICATION

Sustained Activation of Nuclear Erythroid 2-Related Factor 2/Antioxidant Response Element Signaling Promotes Reductive Stress in the Human Mutant Protein Aggregation Cardiomyopathy in Mice

Namakkal Soorappan Rajasekaran,[1] Saradhadevi Varadharaj,[2] Gayatri D. Khanderao,[1] Christopher J. Davidson,[1] Sankaranarayanan Kannan,[3] Matthew A. Firpo,[4] Jay L. Zweier,[2] and Ivor J. Benjamin[1]

Abstract

Inheritable missense mutations in small molecular weight heat-shock proteins (HSP) with chaperone-like properties promote self-oligomerization, protein aggregation, and pathologic states such as hypertrophic cardiomyopathy in humans. We recently described that human mutant αB-crystallin (hR120GCryAB) overexpression that caused protein aggregation cardiomyopathy (PAC) was genetically linked to dysregulation of the antioxidant system and reductive stress (RS) in mice. However, the molecular mechanism that induces RS remains only partially understood. Here we define a critical role for the regulatory nuclear erythroid 2-related factor 2 (Nrf2)-Kelch-like ECH-associated protein (Keap1) pathway—the master transcriptional controller of antioxidants, in the pathogenesis of PAC and RS. In myopathic mice, increased reactive oxygen species signaling during compensatory hypertrophy (*i.e.*, 3 months) was associated with upregulation of key antioxidants in a manner consistent with Nrf2/antioxidant response element (ARE)-dependent transactivation. In transcription factor assays, we further demonstrate increased binding of Nrf2 to ARE during the development of cardiomyopathy. Of interest, we show that the negative regulator Keap1 was predominantly sequestrated in protein aggregates (at 6 months), suggesting that sustained nuclear translocation of activated Nrf2 may be a contributing mechanism for RS. Our findings implicate a novel pathway for therapeutic targeting and abrogating RS linked to experimental cardiomyopathy in humans. *Antioxid. Redox Signal*. 14, 957–971.

Introduction

Inheritable disorders linked to mutations in genes encoding molecular chaperones (*e.g.*, CryAB or heat-shock protein binding factor-2 [HSPB2]) and cytoskeletal proteins contribute to the pathogenesis of heart failure (21–23, 29). Among such pathogenic mechanisms, redox signaling pathways involving glutathione (GSH), a major nonprotein thiol, possess antioxidant properties for detoxifying and scavenging toxic reactive oxygen species (ROS) generated in disease states (25, 26). Paradoxically, we have demonstrated recently that the development of cardiac hypertrophy and heart failure from human R120GαB-crystallin (hR120GCryAB) overexpression caused dysregulation of glutathione homeostasis, termed "reductive stress (RS)," in transgenic mice (TG) (29). Further, quenching of reducing power by inhibiting glucose 6 phosphate dehydrogenase (G6pd) levels/activity and thereby decreasing NADPH rescued the hR120GCryABTG mice from cardiac hypertrophy and cardiomyopathy/heart failure (29). However, the causal mechanism for "RS" remains obscure.

Redox-sensitive transcription factors are attractive candidates whose dysregulation of key molecular targets might contribute to the pathogenic changes in the intracellular redox milieu. Nuclear erythroid 2-related factor 2 (Nrf2; NF-E2-related factor 2) (18), a basic leucine zipper protein, is a redox-sensitive master transcriptional regulator of several cytoprotective genes including the major antioxidants (12, 18, 44). Under basal conditions, Nrf2 is sequestered in the

[1]Division of Cardiology, Department of Internal Medicine, University of Utah Health Sciences Center, Salt Lake City, Utah.
[2]Davis Heart & Lung Research Institute, The Ohio State University, Columbus, Ohio.
[3]Department of Pediatric Research, The University of Texas M. D. Anderson Cancer Center, Houston, Texas.
[4]Department of General Surgery, University of Utah Health Sciences Center, Salt Lake City, Utah.

cytoplasm by the Kelch-like ECH-associated protein (Keap1). Interaction with Keap1 promotes rapid ubiquitination of Nrf2 and subsequent proteasome degradation (18, 27). In response to oxidative or electrophilic stress, Keap1-dependent ubiquitin ligase activity is inhibited and the Nrf2 translocates to the nucleus to induce transactivation of the antioxidant response element (ARE)-containing genes (14, 49). Transcriptional pathways under the control of Nrf2 have been implicated in protection from oxidative stress of vital organs and various diseases such as acute respiratory distress syndrome, hyperoxic injury, pulmonary fibrosis, hepatocellular necrosis, hepatotoxicity, cancer, and neuronal dysfunction (7, 13–19). Using *in vitro* and *in vivo* Nrf2 knockout models, substantial evidence has been developed to support the regulatory role of Nrf2 in antioxidative and cytoprotective functions against pathological conditions, including cancer, pulmonary, inflammatory, and neurodegenerative diseases (4, 9, 18, 28, 32, 33). Thus, Keap1-Nrf2 interaction is an important regulatory nodal point for the overall response to redox stress. Both Nrf2 and Keap1 (a cysteine-rich protein) are redox sensitive proteins (6, 45) and are vulnerable to altered intracellular concentrations of redox couples (*i.e.*, GSH:GSSH, NADPH:NADP, NADH:NAD, −SH:S-S, and cysteine:cystine) (20). Relevant to the cardiovascular system, a recent study has shown that $Nrf2^{-/-}$ mice are susceptible for mechanical pressure overload cardiac hypertrophy, which demonstrates a critical pathophysiological role for Nrf2 in the heart (19).

We identified constitutive activation of Nrf2 in the TG-mouse heart in which human mutant CryAB was overexpressed. Such an activation of Nrf2 is associated with RS and mutant protein aggregation cardiomyopathy (MPAC) in mice. Collectively, these observations suggest that the Nrf2-Keap1 pathway acts as key player in protecting against the mutant protein-induced stress, but eventually contributing to RS, which may be deleterious to the heart. In the current study, we hypothesized that the mutant protein-induced self-oligomerization and formation of insoluble protein aggregates could induce ROS, which can then trigger dissociation of the Nrf2-Keap1 complex, thereby activating Nrf2. We further hypothesized that interactions between the mutant protein aggregates and Keap1 play a key role in stabilization of Nrf2 and activating ARE-dependent cytoprotective mechanisms, which might also lead to RS in the hR120GCryAB TG mouse heart. Since the Nrf2-Keap1 system is crucial for regulating a battery of genes encoding antioxidants and cytoprotective proteins in various oxidative stress disorders, unraveling its direct and key role in heart tissue and cardiovascular pathogenesis will be of potential therapeutic importance. Using the TG mouse model for human heart disease, we have investigated the mechanisms for Nrf2-dependent transactivation of antioxidant genes and resultant RS.

Materials and Methods

Animals

Studies of mice were approved by the Institutional Animal Care and Use Committee at the University of Utah (IACUC No. 08-07006). Nontransgenic (NTG) and hR120GCryAB TG mice in C57/Bl-6 background were generated as previously described (29), and were housed under controlled conditions for temperature and humidity, using a 12-h light/dark cycle. At the indicated time points (3 and 6 months of age), mice were assessed for cardiac hypertrophy by echocardiography.

Antibodies and reagents

The following antibodies and reagents were used: Nrf2-ab (SC-772; Santa Cruz Bio), Keap1 (10503-2-AP; Proteintech), HO-1 (ab13248; Abcam, Inc.), NQO-1 (ab34173), phospho-CryAB (ab5577), glyceraldehyde 3-phosphate dehydrogenase (GAPDH) (ab9485), lamin-B1 (ab16048), super oxide dismutase-1 (SOD-1) (ab13498), Catalase (219010; Calbiochem, Merck kGaA), γ-glutamyl cysteine synthase (γ-GCS) (RB-1697-P1; Labvision/Neomarkers), and mono-/polyubiquitin (BML-PW0150; Enzo Life Sciences). An anti-CryAB polyclonal antibody (Ab) that reacts with mouse and human proteins was raised against 164–175 amino acid residues of human CryAB. Secondary antibodies conjugated with horseradish peroxidase IgG Rabbit and Mouse (PI-1000 & PI-2000; Vector Labs). Radical detecting electron paramagnetic resonance (EPR) probes 1-hydroxy-3-methoxy-carbonyl-2, 2,5,5- tetramethyl pyrrolidine (CMH) (NOX-2.1), TEMPOL (705748; Sigma-Aldrich), EPR grade water (NOX-7.7.1), Krebs-4-(2-hydroxyethyl)-1-piperazineethanesulfonic acid [HEPES] buffer (NOX-7.6.1), diethyl dithio carbomate (DETC) (NOX-10.1), defroxamine (NOX-9.1), glass capillary tubes (NOX-G.3.1), and critoseal (NOX-A. 3.1-VP) were purchased from the Noxygen Diagnostics. Fluorescent probes dihydroethidium (DHE)/dihydro difluro diacetate (H2DCFDA) for detecting ROS and superoxide were obtained from Molecular Probes. Bio-Rad Protein Assay (500-0006; Bio-Rad) was used to determine protein levels in the heart tissue extracts. All reagents and primers for RNA extraction and real-time RT-PCR quantification were purchased from Qiagen, Inc.

Determination of glutathione redox state

Glutathione redox (GSH/GSSG) state was determined in heart tissue extracts from NTG and TG mouse at 3 and 6 months. In brief, heart tissue extracts were prepared in MES buffer and centrifuged at 5000 rpm for 5 min at 4°C. A small aliquot of the supernatants were used for protein determination and the remaining samples were mixed with equal volumes of 10% metaphosphoric acid (Cat. No. 239275; Sigma) to precipitate proteins. A known volume of the metaphosphoric acid extracts was treated with triethanolamine reagent and 2-vinyl pyridine (only for GSSG analysis) and appropriate GSH and GSSG standards were treated similarly to prepare a standard graph. Kinetic GSH-reductase recycling assay was performed following the manufacturer's instructions (703002; Cayman Chemicals) using a plate reader (Bio-Tek; FLx-800) (29, 31).

Determination of tissue redox state and ROS

EPR spectroscopy. To understand the electrophilic signals that are critical to dissociate the Nrf2-Keap1 complex and favor Nrf2 activation, we measured the tissue redox stress/ROS formation and assess the temporal effect of hR120GCryAB expression. Briefly, mice were injected (i.p.) with heparin (4 U/g b.w.) and sacrificed by CO_2 inhalation. Hearts were perfused *in situ* with HEPES buffer (20 μM, pH 7.4) to remove residual blood, a portion of ventricle was cut into small pieces, placed in a clean 24-well tissue culture plate

containing 500 μL HEPES, washed twice, and immersed in 300 μL of the buffer. About 10 mg of processed ventricular tissues was incubated with 150 μL of 500 μM CMH, at 37°C for 30 min. ROS released by tissues react with the CMH to form a stable nitroxide radical that can be measured using electron spin resonance (ESR) (15). Aliquots of the incubated probe media were taken in 50 μL glass capillary tubes and ESR spectra measured using an EMX-ESR spectroscopy (Bruker Instruments) as reported previously (1).

Fluorescent probes (DCFDA/DHE). ROS generation in the mouse myocardial tissue from 3- and 6-month-old NTG and TG mice was determined using DHE/H2DCFDA fluorescence in a manner similar to that reported previously (8, 43). Cytosolic DHE exhibits blue fluorescence; however, when this probe is oxidized to ethidium it intercalates with DNA, staining the nucleus a bright red fluorescence. In the presence of superoxide ($O_2^{-\cdot}$), the cell-permeable nonfluorescent DHE is oxidized to fluorescent 2-hydroxyethidium, which is then detected by using the excitation/emission filters appropriate for rhodamine. H2DCFDA is oxidized by hydrogen peroxide to convert the nonfluorescent DCF to fluorescent DCF, which can be detected by a fluorescent microscope using appropriate excitation/emission filters for fluorescein as reported previously (43). Briefly, at the end of each protocol the hearts were snap-frozen using optimal cutting temperature medium and cut into 5-μm-thick transverse sections placed in clean glass slides. Sections were appropriately covered with the probe solution containing DHE/H2DCFDA (10 μM) along with the nuclear stain DRAQ5 and were incubated in a light-protected chamber at 37°C for 30 min and washed thoroughly with 1×TBS-T thrice, fixed, and mounted using Flouromount-G. Images of the tissue sections were obtained using a Zeiss 510 Meta laser scanning confocal microscope (Carl-Zeiss, Inc.). Fluorescence intensity, which positively correlates with the amount of $O_2^{-\cdot}$ generation, was determined in the myocardial tissue and quantified by automated image analysis using the ImageJ software (National Institutes of Health).

Determination of Nrf2 nuclear translocation: Western blotting

Harvested hearts from 3- and 6-month-old NTG and TG animals were initially flash frozen in liquid nitrogen. Cytosolic lysates from the tissues were prepared by homogenizing the tissue using cytosolic/homogenizing buffer (10 m*M* HEPES, 10 m*M* KCl, 0.1 m*M* EDTA, 0.5 m*M* $MgCl_2$, with freshly prepared 1 m*M* dithiothreitol and 0.1 m*M* phenyl methylsulfonyl fluoride, and 1% Triton×100, pH 7.9), followed by centrifugation at 5200 rpm for 5–6 min. The nuclear pellet was washed with 4 volumes of homogenizing buffer to get rid of any cytosolic contaminants. Nuclear fractions were prepared in complete lysis buffer (20 m*M* HEPES, 420 m*M* NaCl, 0.1 m*M* EDTA, 1.5 m*M* $MgCl_2$, 25% glycerol, 1 m*M* dithiotheitol, and 0.5 m*M* phenyl methylsulfonyl fluoride, pH 7.9). Samples were incubated on ice with mild shaking and centrifuged at 8200 rpm for 8 min. Later, proteins were determined using Biorad Bradford reagent and the samples for Western blots (WB) were prepared in 0.25 volumes of Laemmli buffer with 5% freshly added β-mercapthoethanol and boiled for 5 min. About 30 μg of both nuclear and cytosolic proteins was resolved separately on 10%–12% SDS-PAGE. They were probed using antibodies against CryAB, P-CryAB, Nrf2, HO-1, NQO-1, catalase, Keap1, ubiquitin, SOD-1, γ-GCS, GAPDH, and lamin-B1. Secondary antibodies conjugated with horseradish peroxidase IgG Rabbit and Mouse were used for chemiluminescence detection.

Analysis of Nrf2 binding with ARE by transactivation assay

The level of Nrf2 activation and DNA binding efficacy at the RS state was evaluated in the NTG and TG mouse hearts using Trans AM Nrf2 Kit (50296; Active Motif). About 10 μg of nuclear proteins was incubated with immobilized oligonucleotide containing ARE consensus binding site (5′-GTCACA GTACTCAGCAGAATCTG-3′) and the active form of Nrf2 that bound to the oligo was detected using anti-Nrf2 primary Ab recognizing epitope on Nrf2 protein after treating with HRP-conjugated secondary Ab. The resultant chromogen formed due to the specific activity of the transcription factor in the nuclear extracts was read in a plate reader. Absorbance at 450 nm was expressed as the direct activity of Nrf2.

Determination of Nrf2 ubiquitination and interaction with Keap1

Since Keap1 regulates the fate of Nrf2 ubiquitination and stabilization in cytoplasm, we have analyzed the ubiquitin-conjugated Nrf2 by immunoprecipitation (IP) using ubiquitin Ab, followed by WB against anti-Nrf2 Ab. Briefly, 200 μl of 0.5 mg/ml cytosol proteins from NTG and TG mouse hearts was incubated with an anti-ubiquitin Ab (for 12 h at 4°C with gentle rotation) and protein-A/G agarose beads (Invitrogen Corporation) and washed the precipitates thoroughly in wash buffer. IP proteins were analyzed by WB with an anti-Nrf2 Ab. Further to investigate the degree of Nrf2-Keap1 association, we performed IP from the cytosol extracts with anti-Keap1 Ab and probed with anti-Nrf2 Ab.

RNA isolation, reverse transcription, and gene expression using quantitative real-time PCR

Hearts were harvested after *in situ* perfusion with 10 ml of RNase free PBS and 10 ml of *RNA later* reagent. To extract RNA, ~30 mg of ventricular tissue was processed from 3- and 6-month-old NTG and TG mice ($n = 5$) using RNA extraction kit (Qiagen; Cat. No. 74106) following supplier's instructions. RNA samples were then quantified by measuring the absorbance at 260 nm. Reverse transcription reaction was performed using 2.5 μg RNA using Qiagen Reverse Transcription Kit (Cat. No. 205311) as per manufacturer's instructions to synthesize cDNA using oligo(dT). For quantitative real-time RT-PCR analysis, 100 ng of cDNA template, 10 μL of SYBR green master mix (Qiagen; Cat. No. 204054), and respective Qiagen primer sets for *HO-1* (QT00095270), *NQO-1* (QT00094367), *catalase* (QT01058106), *G6pd* (QT00120750), glutamyl cysteine ligase (catalytic) *(GCLC)* (QT QT00130543), glutamyl cysteine ligase (modulatory) *[GCLM]* (QT00174300), *Nrf2* (QT00095270), and *Keap1* (QT00147371) were used and analyzed in a Light Cycler real-time thermocycler (Roche Bio). Copy numbers of cDNA targets were quantified using Ct values and the messenger RNA (mRNA) expression levels for all samples were normalized to the level of the housekeeping gene *Arbp1* (QT00249375) or *GAPDH* (QT01658692).

Determination of Keap1 sequestration and colocalization with the mutant CryAB protein aggregates by immunofluorescence and IP/WB

Frozen sections at 5 μm thickness were obtained from the 3- and 6-month-old NTG and TG mice hearts to localize Keap1/CryAB by immunostaining method as reported previously (42). The sections attached to the cover slips were fixed with 3.7% paraformaldehyde for 10 min, permeabilized with 0.25% Triton X-100 in TBS containing 0.01% Tween-20 for 5 min, and blocked for 30 min with 1% BSA in 0.01% tris buffered saline-Tween-20 (TBST) and incubated with primary anti-CryAB/Keap1 at a dilution of 1:2000 and 1:500, respectively, in 0.01% TBST containing 1% BSA for 1 h at room temperature. After treatment of sections with the chosen primary antibodies, they were incubated with secondary anti-rabbit Alexa Fluor 488–conjugated and secondary anti-mouse AlexaFluor 586–conjugated antibodies (1:1000 dilution), wherever necessary, for 1 h at room temperature. After thorough washing with 1×TBS-T the sections were mounted with the antifade mounting medium (Fluoromount-G) and viewed with 510 Meta Zeiss Confocal (Carl-Zeiss, Inc.) microscope at a magnification of 60×for observation of specific localization and interactions between CryAB and Keap1 proteins. WB analysis was done on the cytosolic fraction of the respective mouse hearts to confirm the active Keap1 protein levels at 3 and 6 months of age. Further, we performed IP with anti-CryAB-ab followed by WB with anti-Keap1-ab to indentify and quantify the interactions between the Keap1 and mutant CryAB in supernatant (cytosolic) and pellet (cytoskeletal & nuclear) fractions of NTG and TG mouse hearts at 6 months of age.

Statistical methods

Data are expressed as mean ± standard deviation. Analysis of variance followed by the Student–Newman–Keul multiple comparison tests was used to determine the significant differences between the groups. p-Values <0.05 were considered significant.

Results

Heart-specific overexpression of mutant-CryAB triggers cardiac hypertrophy along with RS

We have recently reported that moderate overexpression of the missense human R120G mutant CryAB associated with protein aggregation causes cardiomyopathy and dysregulation of glutathione homeostasis, termed RS (29, 30). We have repeated these experiments to validate our previous findings in the hR120GCryAB TG overexpressors in 3- and 6-month-old mice that were subsequently used for Nrf2 studies. We determined heart-to-body weight ratios and found no differences between the NTG and TG at 3 months, but the heart-to-body weight ratio was significantly increased for mutant CryAB-TG compared with NTG mice at 6 months (Fig. 1A, B). Given that cardiac hypertrophy occurred in these hearts at 6 months, we next assessed the major intracellular thiols,

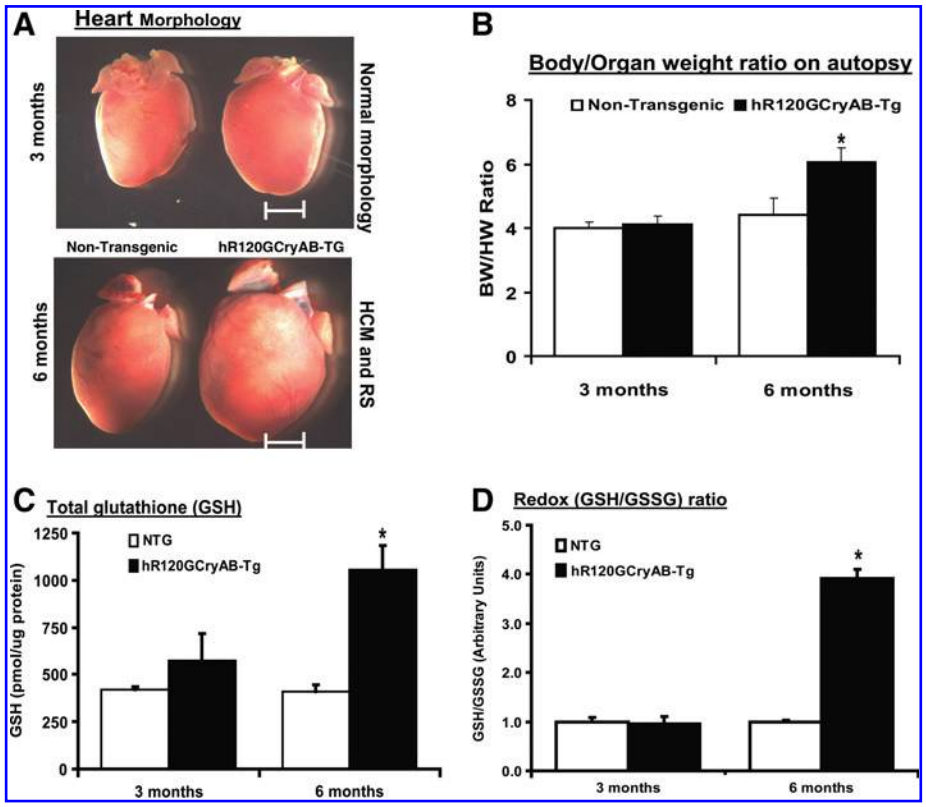

FIG. 1. Tissue-specific transgenic (TG) overexpression of human mutant αB-crystallin (hR120GCryAB) induces hypertrophic cardiomyopathy in mice. (A) Heart-specific overexpression of mutant protein induces pathological ventricular hypertrophy and biatrial thrombosis at 6 months of age. No such phenotypical (hypertrophy) changes and cardiac dysfunction are evident in the 3-month-old mice. **(B)** Organ-to-body (heart/body) weight ratios on autopsy confirm the cardiac hypertrophy in the hR120CryAB-TG mouse at 6 months of age but not in the 3-month-old mice. $n=8$ or more mice from each group ($p<0.01$). **(C, D)** Redox markers (GSH and GSH/GSSG): Determined the concentrations of reduced and oxidized glutathione in non-transgenic (NTG) and TG mouse heart ventricles ($n=4$) at 3 and 6 months. At 3 months, no statistically significant change in GSH levels was recorded among the experimental groups. Dramatic increase in GSH and GSH/GSSG redox ratio was evident in the TG mouse at 6 months, indicating highly enhanced reducing environment along with pathological hypertrophy. Values are mean + standard deviation for 4 or animals in each group (*$p<0.01$). (For interpretation of the references to color in this figure legend, the reader is referred to the web version of this article at www.liebertonline.com/ars).

reduced (GSH), and oxidized (GSSG) glutathione ratios, for evidence of redox imbalance linked to the pathogenic events. Interestingly, we found similar intracellular GSH levels between the NTG and TG at 3 months, but these values were significantly increased in the TG mouse hearts at 6 months along with profoundly increased GSH/GSSG ratios (Fig. 1C, D). Since the TG hypertrophied hearts exhibit enhanced reducing power, we tested the hypothesis that Nrf2, a master transcriptional regulator of numerous antioxidants/cytoprotective genes, played a role in pathogenic redox imbalance (18).

Mutant protein overexpression induces ROS generation

Apart from basal nuclear expression of Nrf2 under unstressed conditions (18), increased production of ROS, RNS, and other electrophile chemical species induces Nrf2 activation and its nuclear translocation (32, 34, 37, 41). To quantify the redox stress and ROS formation, we utilized EPR spectroscopy with redox-sensitive spin probes (Fig. 2). With the spin probe CMH that in the presence of ROS is oxidized to form its EPR detectable nitroxide radical, a prominent increase in radical formation is seen in the TG compared to NTG myocardium at 3 months, but these signals are not distinguishable at 6 months (Fig. 2A, B). We next determined the levels of ROS using two independent fluorescent probes (DCFH-DA/DHE) of NTG and TG hearts at 3 and 6 months, respectively (Fig. 2C–E). These results confirmed that increased ROS formation occurs in 3-month-old TG compared to NTG mice, suggesting the development of oxidative stress in the TG mice at 3 months. In contrast, at 6 months no increase was seen in the TG compared to the NTG myocardium, suggesting that reductive compensation may occur.

Together, these results are consistent with the notion that alterations of ROS might underlie early activation of signaling cascades, including Nrf2-Keap1 pathway and contribute to subsequent development of pathologic cardiac hypertrophy and GSH imbalance *in vivo*. Next, we have assessed whether this apparent excess ROS generation in the TG hearts had direct consequence on Nrf2 nuclear translocation and transactivation of key antioxidants.

Increased ROS causes sustained nuclear translocation of Nrf2 in the TG mouse expressed with mutant protein

Under physiological conditions, Nrf2 is tethered to its cytosolic partner, Keap1 and degraded by the ubiquitin/proteasome pathway (32, 37). In turn, the release of Nrf2 from its negative regulator translocates into the nucleus, binds to recognition sequences, and mediates the transcriptional activation of downstream target genes. We hypothesized that increase in ROS signaling by hR120GCryAB expression would induce Nrf2 nuclear translocation during compensatory hypertrophy. To determine the intracellular localization of Nrf2, we isolated cytosolic and nuclear fractions from NTG and TG myocardium and performed WB analysis using Nrf2-Ab. We found that Nrf2 expression in the nuclear fraction was eight- and sixfold higher in TG compared with NTG at 3 and 6 months, respectively (Fig. 3A, C, D, F). This prominent nuclear translocation of Nrf2 was coupled with nuclear translocation of mutant CryAB and its phosphorylated form in the TG mouse heart (Fig. 3A, B, D, E). These results suggest that hR120GCryAB expression increases translocation of Nrf2 into the nucleus of TG compared with NTG mice.

Nuclear translocation of Nrf2 results in its enhanced ARE binding activity in the TG mouse

Next, to investigate the consequent function of Nrf2 in the hypertrophy hearts, we determined the Nrf2 activity using ARE-oligonucleotide-based transactivation assay in the nuclear extracts of NTG and TG mouse hearts at 6 months of age. The Nrf2 activity was significantly higher (>2.0-fold) in the TG mouse hearts, suggesting its activation along with increased antioxidant capacity (Fig. 4A). To further confirm these results, we have analyzed ubiquitination of Nrf2 in the NTG and TG mouse at 3 and 6 months. Of interest, IP/Co-IP experiments detected significantly lower ubiquitination of Nrf2 in the TG heart extracts (Fig. 4B) than the NTG, indicating that possible dissociation of Nrf2 from its cytosolic negative regulator, Keap1, in TG mouse is consistent with elevated nuclear translocation seen in Figure 3. IP of Keap1 and followed by WB with anti-Nrf2-Ab revealed poor interactions of these proteins in the cytosol of TG mouse when compared with NTG (Fig. 4C), suggesting dissociation of the Nrf2/Keap1 complex and thereby decreased the ubiquitination of Nrf2 as shown in Figure 4B. Taken together, these results indicate that significant dissociation of Nrf2/Keap1 complex prevented proteasomal degradation of Nrf2 and promoted its activation/nuclear translocation in the TG hearts.

Sustained activation/nuclear translocation of Nrf2 in the TG mice upregulates transcription of ARE containing antioxidant genes

We hypothesized that increased translocation and DNA-binding activities of Nrf2 might induce transcriptional activation of downstream targets, including critical antioxidative pathways associated with glutathione homeostasis. To test this hypothesis, we performed real-time RT-PCR using RNA isolated from the 3- and 6-month-old NTG and TG mouse hearts. We selected several potential target genes under the control of NRF2/ARE-dependent regulation, including the major antioxidant genes. *Catalase* (Fig. 5G), *G6pd* (29, 30), and NADH-quinone oxidase (Nqo1) were significantly upregulated in the TG compared with NTG mouse hearts at 3 months (Fig. 5A), suggesting that onset of compensatory mechanisms against mutant CryAB induced cardiac hypertrophy. Expression was elevated for *Gclm, Gclc,* and hemoxygenase-*1 (Ho1)* in the TG mouse compared with NTG, but these changes did not reach the level of significance (Fig. 5B–F). In 6 months' hearts, demonstrating cardiac hypertrophy, the antioxidant genes *Nqo1*, *Ho1*, *G6pd*, *catalase*, *Gclm*, and *Gclc* were significantly upregulated in TG compared to NTG hearts (Fig. 5I–O). Although mRNA levels for Nrf2 did not altered significantly at 3 months, there was an increasing trend ($p < 0.072$) at 6 months in TG compared to age-matched NTG mice (Fig. 5M), indicating that there might be ARE-dependent transcriptional upregulation of *Nrf2* gene. ARE-mediated auto-regulation of Nrf2 has been reported previously (17).

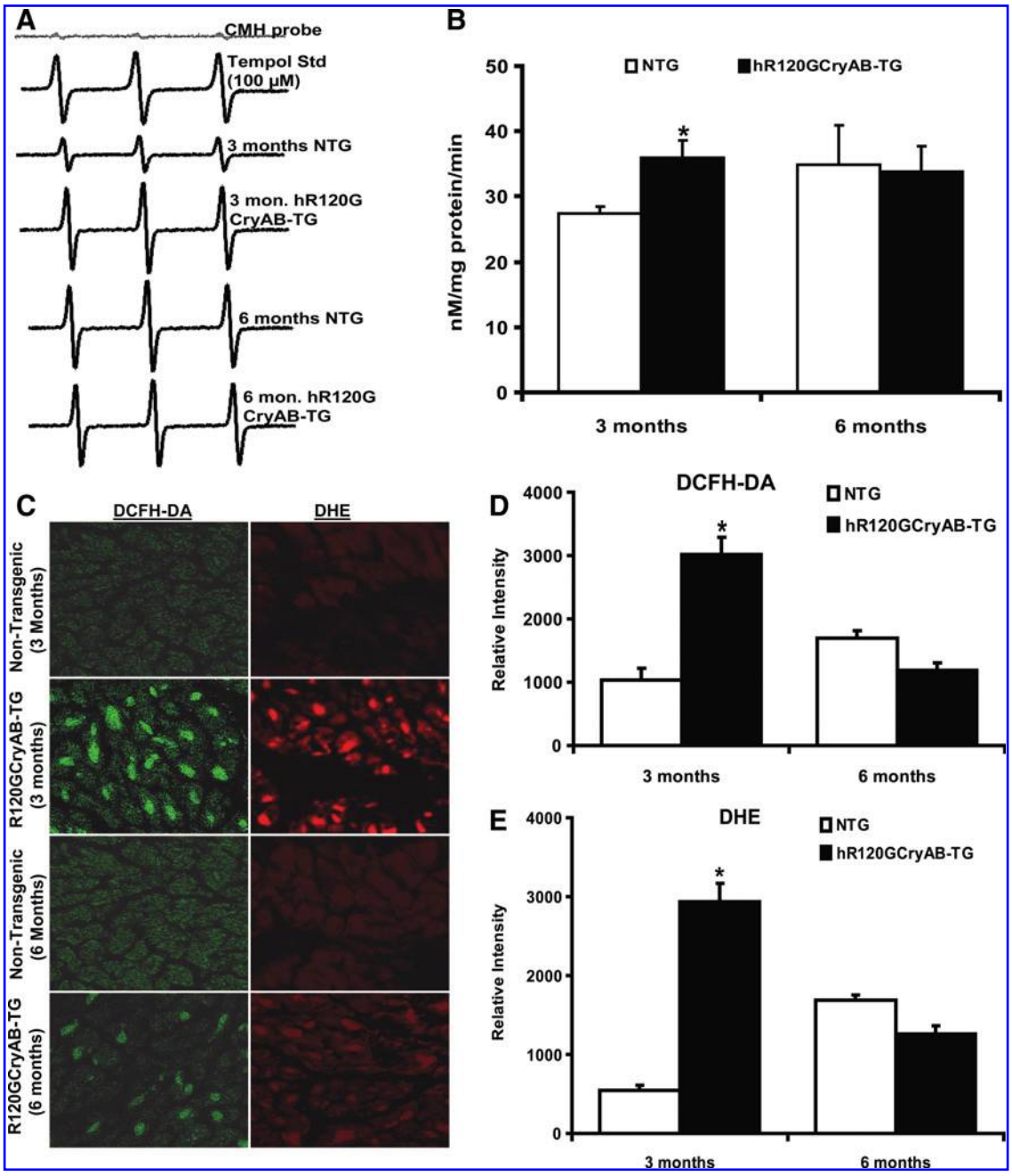

FIG. 2. Total reactive oxygen species (ROS) formation is enriched in myocardium of the TG mouse heart at 3 months but not at 6 months. (A) Electron paramagnetic resonance (EPR) signals for 1-hydroxy-3-methoxycarbonyl-2,2,5,5-tetramethylpyrrolidine (CMH) in the NTG and TG mouse heart tissues. Representative EPR signals for CMH showing prominent differences between the NTG and TG hearts with higher radical generation in the TG at 3 months but no significant difference after 6 months. **(B)** Graph of the radical formation in the ventricular tissue determined using CMH spin probe. Significantly increased radical formation is evident in the 3-month-old TG mouse hearts compared with the NTG ($^*p < 0.05$). However, the ROS levels were not significantly different between the NTG and TG at 6 months. **(C–E)** Determination of ROS in the myocardial tissue sections using fluorescent (dihydro difluro diacetate [H2DCFDA]/dihydroethidium [DHE]) probes. **(C)** Staining with DCFDA/DHE: Determination of ROS using fluorescent probes (H2DCFDA/DHE) and microscopy. Frozen tissue sections were incubated with 10 (*M* of H2DCFDA/DHE for 30 min at 37°C. Sections were then washed with 1×PBS, mounted and analyzed by Zeiss 510 Meta confocal microscopy. Significantly increased ROS levels were seen in the TG mouse heart compared with NTG at 3 months ($p < 0.01$), but these values were insignificant at 6 months of age, suggestive of a more highly reduced environment **(D, E)**.

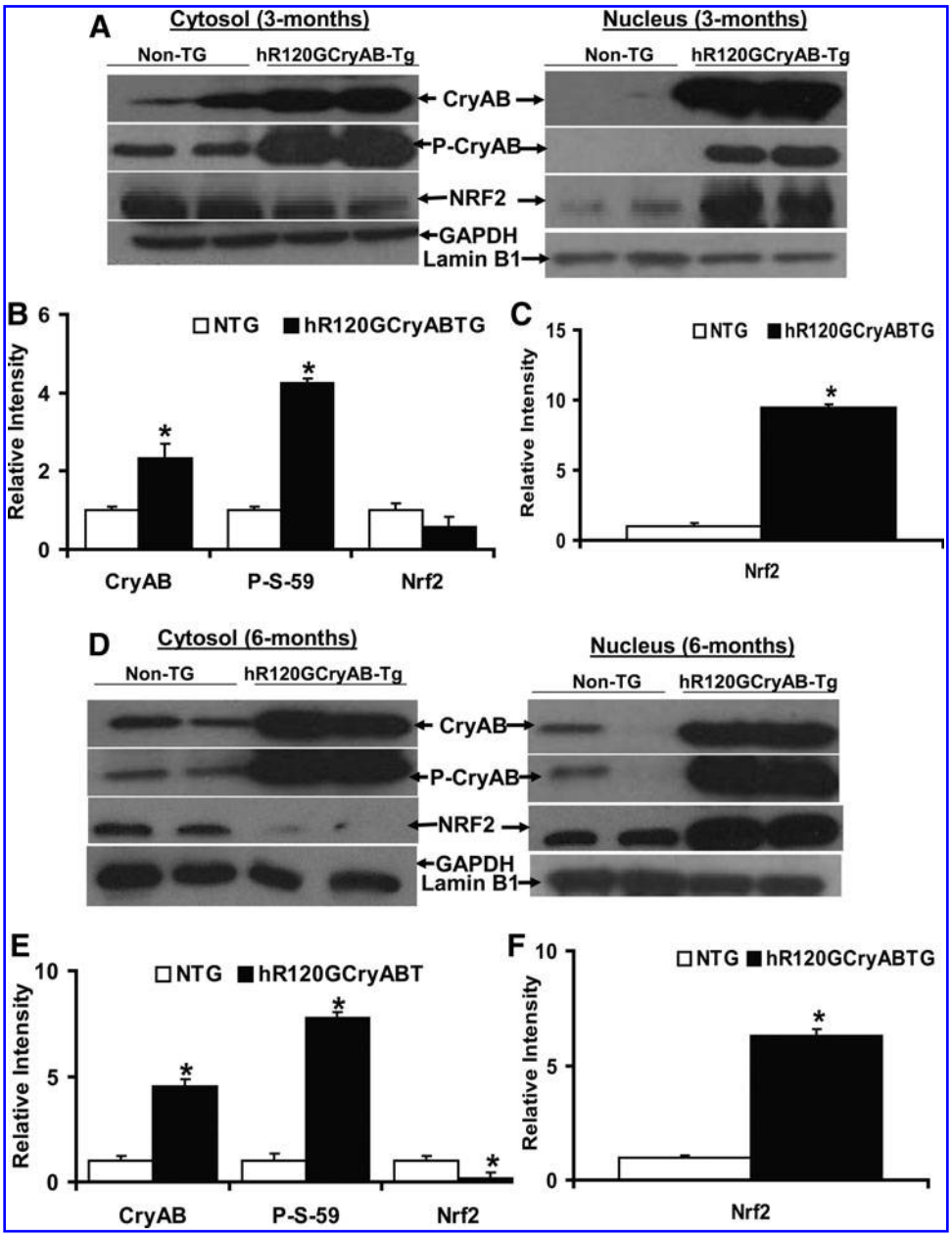

FIG. 3. Nuclear translocation of nuclear erythroid 2-related factor 2 (Nrf2) is prominent in the TG mice overexpressed with mutant CryAB at 3 and 6 months of age. (A) Representative Western blots (WBs) of cytosolic and nuclear fractions obtained from 3-month-old NTG and mutant CryAB (TG) mice. Each lane indicates an individual mouse. Along with abundant expression of mutant protein (nonphosphorylated/phosphorylated forms), the nuclear translocation of Nrf2 is predominant in the TG mouse heart. **(B)** Densitometry analysis for CryAB and P-(S59)-CryAB reveals 3- and >4-fold increase, respectively, in the cytosol of TG mice compared to the NTG. A significant (~50%) reduction of Nrf2 in the cytosol of TG mice is evident (*$p < 0.01$). **(C)** Obviously, the nuclear translocation of Nrf2 is highly significant (~8-fold) in the TG compared to the NTG mice **(C)**. Densitometry analysis was not performed for mutant CryAB (phosphorylated and nonphosphorylated forms) due to their exclusive presence in the nuclear fraction of TG mice. **(D)** Representative WBs of cytosolic and nuclear fractions obtained from 6-month-old NTG and mutant CryAB (TG) mice. Each lane indicates an individual mouse. Along with abundant expression of mutant protein (nonphosphorylated/phosphorylated forms) Nrf2 is translocated into the nucleus in the TG mouse heart. **(E)** Densitometry analysis for CryAB and P-(S59)-CryAB reveal ~5- and >8-fold increase, respectively, in the cytosol of TG mice compared to the NTG at 6 months of age. A huge reduction (~90%) of Nrf2 in the cytosol of TG mice is evident, whereas significant Nrf2 nuclear translocation is also evident in the NTG at 6 months, indicating age-associated activation. As expected, nuclear translocation of Nrf2 is prominent (~6-fold when compared to NTG) in the TG mouse heart at 6 months, suggesting sustained nuclear translocation of Nrf2 during the pathogenesis of cardiomyopathy **(F)** (*$p < 0.01$).

Nrf2-dependent upregulation of transcriptional machinery is associated with increased antioxidant protein expression

To characterize whether the Nrf2 activation, in part, was responsible for the increased GSH levels and RS in the TG mouse heart (29), we measured protein expression for the major targets of Nrf2 and enzymes that are involved in GSH metabolism. The WB analysis in either cytosol or nucleus showed dramatic increase in various antioxidants (Fig. 6). At 3 months of age, Nqo1 (>2.0-fold), Ho1 (2.0-fold), and catalase (~4.0-fold) were significantly increased and sod-1 was decreased (50%) in TG hearts related to NTG animals. Unexpectedly, increased catalase did not effectively quenched H_2O_2 (DCFH-DA), which could be due to superoxide-mediated inactivation of catalase in TG mice. It has been previously shown that superoxide radicals could inhibit catalase (16). Interestingly, at 6 months majority of the antioxidants (catalase, G6pd, glutathione peroxidase-1 [Gpx1], and glutathione reductase [Gsr]) (29, 30) and Nqo1 were increased significantly. These results are consistent with those of RT-PCR and indicate that the activation of Nrf2 is strongly associated with significant upregulation of GSH metabolic enzymes and proteins as compensatory mechanisms against

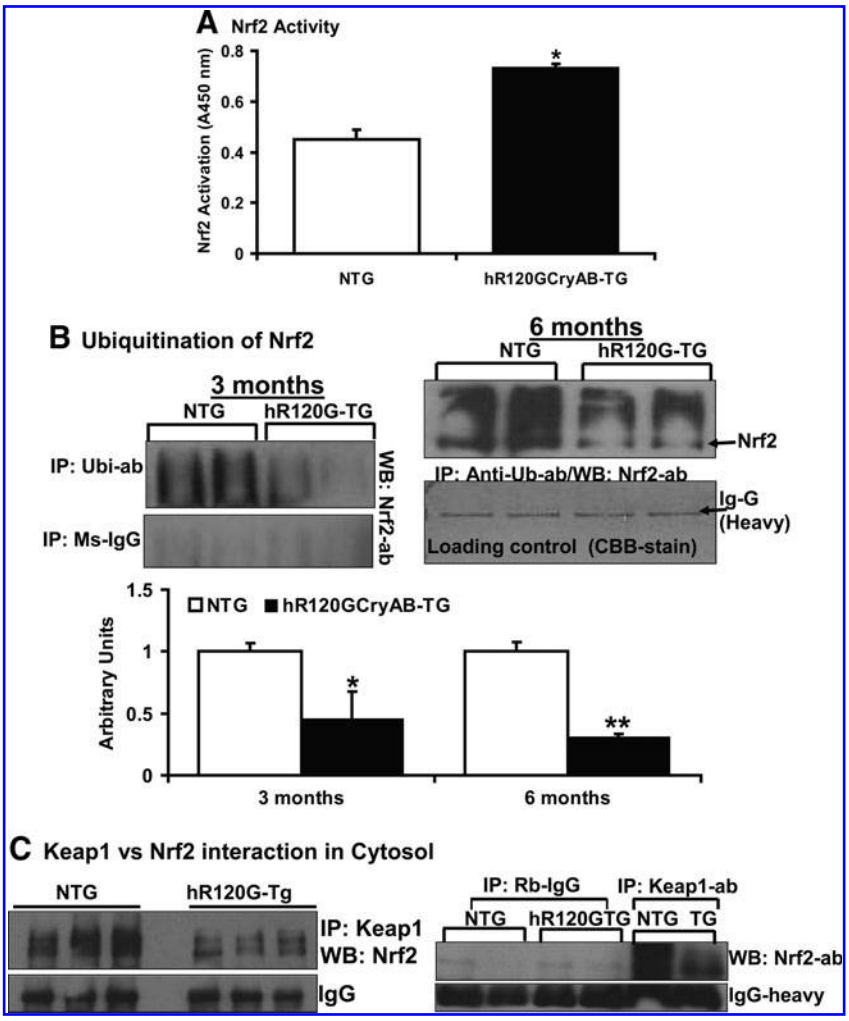

FIG. 4. Decreased ubiquitination and increased activity of Nrf2 in the TG mouse. (A) TransAM-Nrf2 activity assay: Nuclear extracts from NTG and TG mouse ($n = 6$) at 6 months were incubated with the precoated antioxidant response element (ARE) oligonucleotides. Using ant-Nrf2-ab and HRP-conjugated secondary, specific activity for Nrf2 was measured in a plate reader. Results were expressed as A450 nm ± standard deviation for four mice in each group ($^*p < 0.05$). **(B)** Ubiquitination of Nrf2: Representative immunoprecipitation (IP) (with poly-ubiquitin-ab) and WB (with anti-Nrf2-ab) analysis performed in NTG and TG cytosolic fractions indicating decreased ubiquitination of Nrf2, suggesting its enhanced nuclear translocation in the TG mouse at 3 and 6 months ($^{**}p < 0.01$). **(C)** Nrf2 interaction with Kelch-like ECH-associated protein (Keap1): Representative WB analysis showing poor interactions between the Keap1 and Nrf2 in the TG mice compared with NTG and this observation is in line with decreased ubiquitination and enhanced nuclear translocation of Nrf2. Rb-IgG was used as control to perform IP with NTG/TG samples.

pathogenesis of mutant CryAB-induced protein aggregation in the TG mice (Fig. 6A–D). However, no change in the protein levels of γ-GCS, the rate-limiting enzyme for GSH biosynthesis, was observed at either 3 or 6 months of age, indicating possible feed back inhibition on its production/catalytic function. It is conceivable that upon onset of protein aggregation and ROS generation in the TG mouse, there might be possible increased recruitment/utilization of antioxidants to compensate the stress induced by mutant protein overexpression at 3 months than 6 months of age.

Sequestration of Keap1 with mutant protein aggregates facilitate Nrf2 activation

Immunofluorescence analysis (Fig. 7) performed in heart cryosections indicated that Keap1 (red) is colocalized with mutant CryAB (green) aggregates (yellow). Although endogenous CryAB (green) and Keap1 (red) were observed, no prominent interactions (colocalization) of CryAB and Keap1 were evident in the Nrf2-KO mouse heart (Fig. 7A). At 3 months, minimal interactions between the Keap1 and mutant protein (anti-CryAB-Ab) were evident. Along with the increased ROS as determined by EPR, colocalization of Keap1 into the tiny protein aggregates might diminish its potential interactions with Nrf2 (Fig. 7C; inset arrows). Obviously, at 6 months the majority of the Keap1 was bound to the protein aggregates in the TG mouse heart (Fig. 7E; inset arrows), indicating its poor ability to interact with Nrf2, which might explain the sustained nuclear translocation and increased activity of this transcription factor. Inset boxes in each panel showing magnified view (100 μm) of the Keap1-CryAB colocalization with the aggregates (yellow on merged images).

Keap1 interacts with mutant CryAB in 6-month-old myopathic hearts

To determine the effects of mutant CryAB expression on the negative regulator Keap1, we obtained cardiac extracts and probed for the levels of Keap1 in cytosol from NTG and TG mouse at 3 and 6 months. Although protein levels of Keap1 were unchanged between NTG and TG at 3 months, we found a significant decrease (50%) of Keap1 protein in cytosolic fractions in the TG compared to NTG at 6 months (Fig. 8A, B). Further, our results from IP and WB analyses revealed prominent and strong interactions between the Keap1 and mutant CryAB in TG mouse when compared with NTG (Fig. 8C). These robust interactions were confirmed by immunohistochemistry (Fig. 7E; inset box) in which Keap1 appears sequestered into the mutant CryAB aggregates of hR120GCryAB hearts.

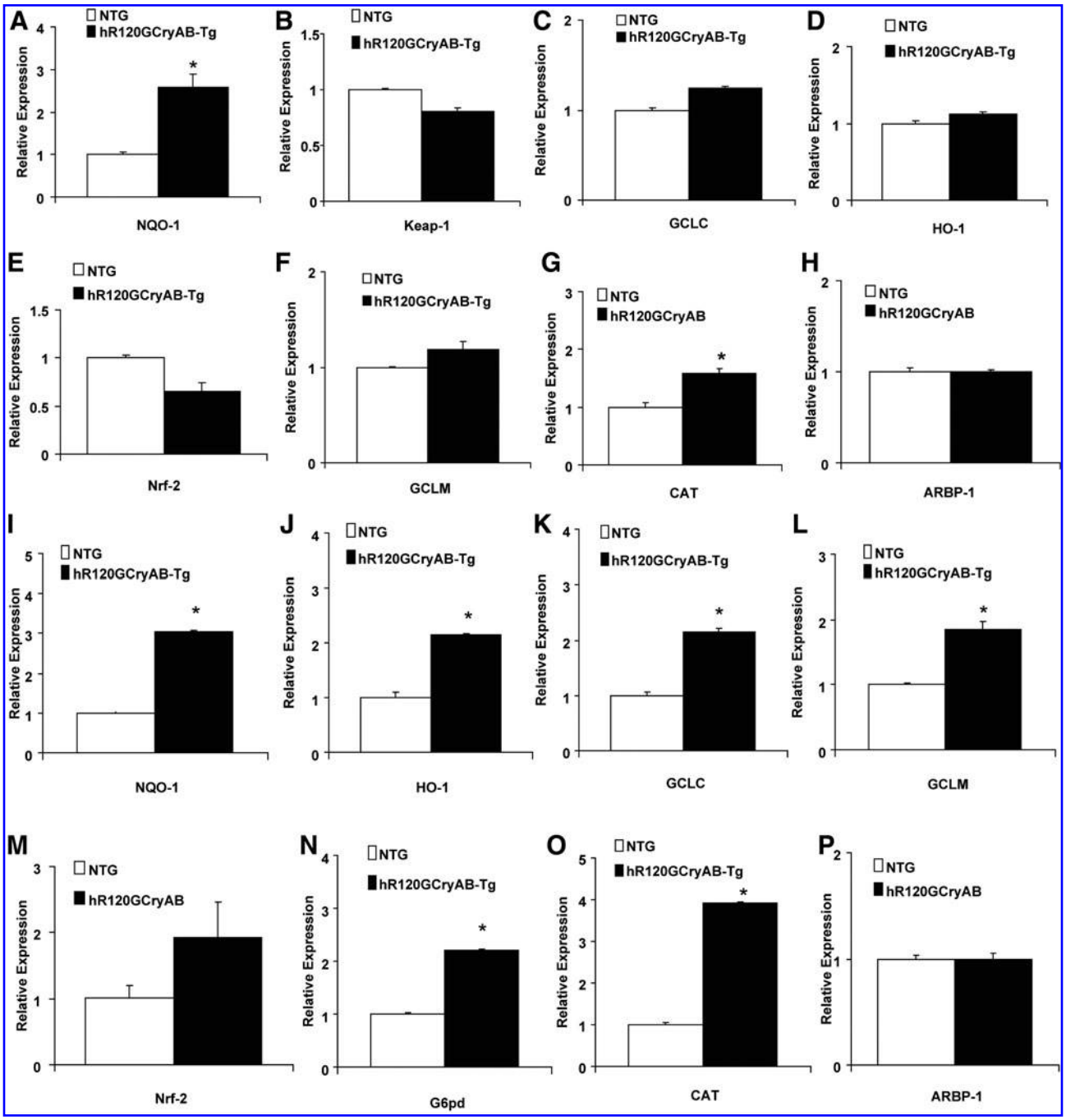

FIG. 5. Sustained Nrf2 nuclear translocation in the TG hearts induces gene expression of ARE-dependent antioxidants. Real-time RT-PCR determinations of Nrf2 target genes in NTG and TG mouse at 3 **(A–H)** and 6 months **(I–P)** were performed using Qiagen-mouse primer sets ($n \geq 6$). Data were first normalized to *Arbp1* expression and then to the corresponding gene expression in the NTG group (Delta-delta-CT method). While there is an increasing trend in the messenger RNA (mRNA) expression for major targets of Nrf2, *catalase* ($\sim$5-fold increase) and NADH-quinone oxidase *(Nqo1)* genes were significantly upregulated at 3 months **(A)**. At 6 months, most of the major antioxidant genes (*Nqo1*, *catalase, hemoxygenase-1 [Ho1],* glutamyl cysteine ligase (modulatory) *[Gclm],* glutamyl cysteine ligase (catalytic) *[Gclc],* and glucose 6 phosphate dehydrogenase *[G6pd]*) were significantly upregulated **(I–P)** to facilitate the highly reduced environment ($^*p < 0.05$ *vs.* NTG).

Discussion

Our findings identify Nrf2-Keap1 pathway as a critical regulator of cardiac defense system and demonstrate the contributing mechanism for RS in the MPAC. An imbalance in the redox equilibrium toward an increase in ROS and oxidative stress has been implicated in the pathophysiology of multiple cardiovascular diseases, including cardiac hypertrophy and cardiomyopathy (5, 7, 31, 40). Surprisingly, we have discovered recently that the "RS" is associated with the molecular pathogenesis of MPAC in the hR120GCryAB TG mouse heart (29). Our observations are consistent with links

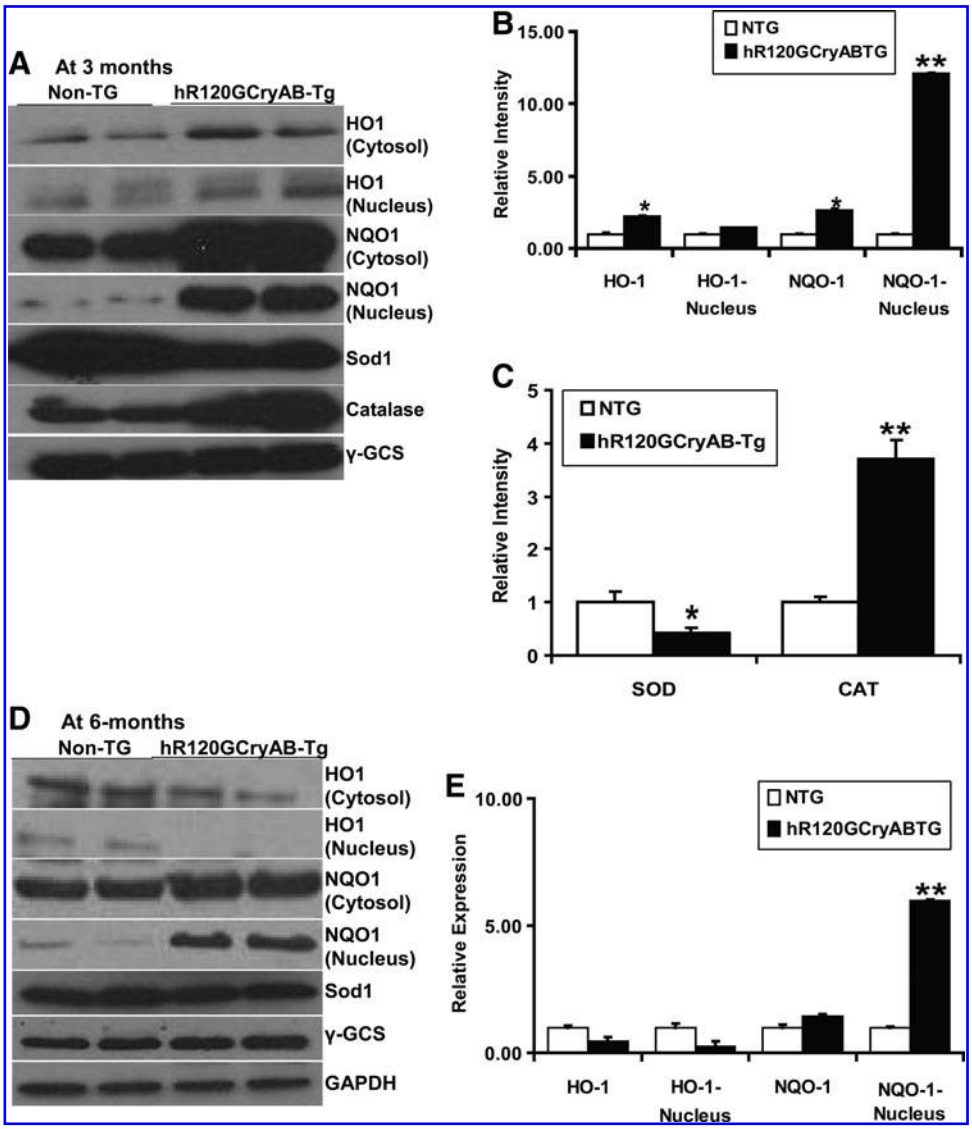

FIG. 6. Increased transactivation of key antioxidant genes in the TG hearts induces their protein expression at 3 and 6 months. (A, D) Representative WB experiments of cytosol or nucleus from NTG and TG mice at 3 and 6 months, respectively. Protein blots were probed with anti-Ho1, Nqo1, super oxide dismutase-1 (Sod-1), catalase, and γ-Gcl. Each lane indicates an individual mouse. **(B, C, E)** Densitometry analysis were performed as relative intensity values calculated as mean arbitrary units obtained from the WB shown in **(A)** and **(D)**, respectively ($^{*}p < 0.05$, $^{**}p < 0.01$, *vs.* NTG). Significant increases in the Ho1 and Nqo1 in the cytosol and Nqo1 in the nucleus of TG mice were evident at 3 months. At 6 months, Ho1 protein is decreased, whereas the same increasing trend exists with the Nqo1 protein expression in the cytosol and nucleus of TG mice in association with reductive stress.

between mutant-protein-induced ROS, and sustained Nrf2 nuclear translocation occurs at 3 months along with onset of cardiac hypertrophy. Further, such activation of Nrf2 is prominent at 6 months with cardiac hypertrophy and RS due to surpassing sequestration of Keap1 in the mutant-CryAB aggregates. Thus, the mechanisms for Nrf2 activation in the MPAC occur at two stages: initially due to ROS generation, and later due to Keap1 dysfunction through its sequestration into the mutant protein aggregates. These results strongly support our hypothesis that "sustained activation and nuclear translocation of Nrf2 in the hR120GCryAB mouse heart will lead to ceaseless transcriptional upregulation of antioxidants contributing to RS."

Mutant protein-induced ROS generation favors Nrf2-Keap1 dissociation on or before the onset of cardiac hypertrophy

Previous reports have authenticated that the ROS and electrophilic stress could be the primary trigger for the dissociation of Keap1-Nrf2 complex and consequent activation of Nrf2 (3, 13, 14). Our multiple observations reveal sustained activation/translocation of Nrf2 into the nucleus of MPAC mouse heart. A fundamental question addressed in this study is whether the mutant-CryAB aggregates could trigger ROS generation in the mouse heart. Previous studies have documented direct evidence that β-amyloid protein aggregates generate hydrogen peroxide and ROS in Alzheimer's disease (10, 38, 39). Here we show that increased ROS/superoxide were generated in the TG mouse heart at 3 months of age with no evidence of cardiac hypertrophy. These observations suggest that there could be an ROS-mediated dissociation of Keap1-Nrf2 complex in the TG mouse at 3 months age as previously demonstrated in other models of Nrf2-dependent protection (3, 14, 18, 19). An important interpretation of these results might be that the mutant-protein that forms self-oligomers is toxic to intracellular environment; in other words, such toxic events could generate ROS, which then would challenge the intracellular defense system (2, 29, 30, 38, 46). At 3 months of age, our results demonstrate that Nrf2 is

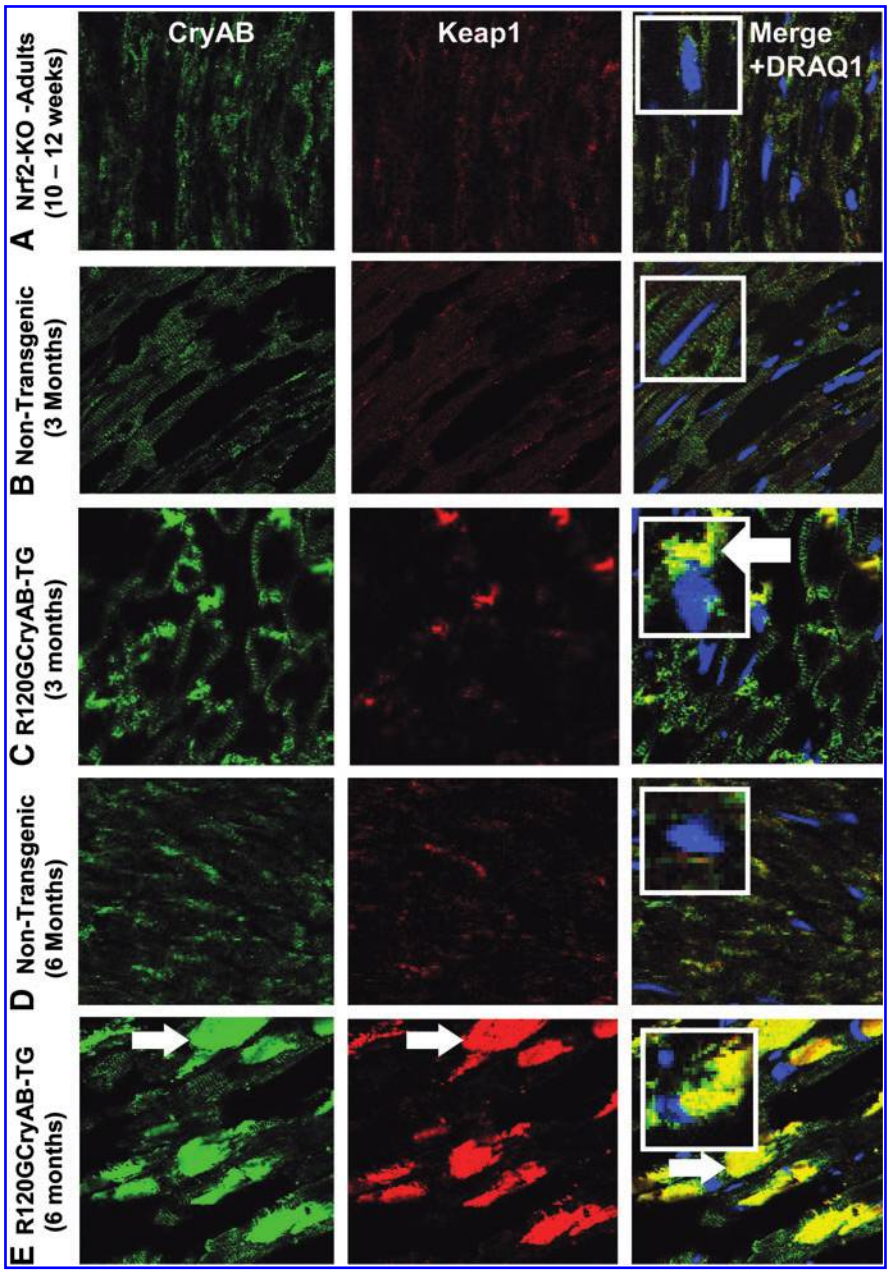

FIG. 7. Sequestration of Keap1 in to the mutant CryAB aggregates facilitate Nrf2 nuclear translocation. Immunofluorescence analysis was performed using the CryAB (Rb.ab, green) and Keap1 (SC-Goat ab, red) and merged with the nuclear staining (DRAQ1). CryAB and Keap1 were colocalized around the perinuclear area of neither Nrf2-KO nor NTG mouse hearts **(A, B, D)**. Prominent colocalization of these proteins is evident in the R120G CryAB-Tg at 3 and 6 months of age **(C, E)**. Robust interactions could be observed in 6-month-old TG mice, indicating that the Keap1 is sequestered into the aggregates, which favors sustained dissociation and stabilization of Nrf2. *Inset arrows* and *boxes* in each *panel* showing magnified view (100 μm) of the Keap1-CryAB colocalization with the aggregates (yellow on merged images).

activated and translocates into the nucleus, which may be attributed to increased ROS generation in the TG mice as evident from the EPR and fluorescent microscopy analysis.

While Nrf2 is activated before the onset of cardiac hypertrophy, the precise mechanism for its sustained nuclear translocation is of particular interest. To understand this aspect, we measured ROS formation in the hR120GCryAB mouse heart at 6 months of age using similar EPR analysis. Interestingly, we observed that there are no significant differences in ROS formation between the control (NTG) and TG mouse hearts, indicating a potential shift in the intracellular redox milieu toward a reductive state. In fact, our previous studies have documented that at 6 months, the intracellular reducing power (glutathione and NADPH) is significantly increased (termed as RS) along with diminished protein carbonylation/lipid peroxidation in the MPAC mouse (29). Although there is strong evidence for initial activation of Nrf2 *via* increased ROS generation at 3 months of age, unraveling the mechanism for its sustained activation at 6 months is important to understand the progression of RS.

Sequestration of Keap1 into the mutant protein aggregates facilitate sustained activation/nuclear translocation of Nrf2 in the MPAC

A significant finding of this study is that misfolded proteins such as mutant CryAB play a key role in the activation of Nrf2/ARE pathways by sequestering the Keap1 into protein aggregates. Our immunofluorescence findings reveal prominent colocalization of Keap1 with the mutant CryAB in the TG

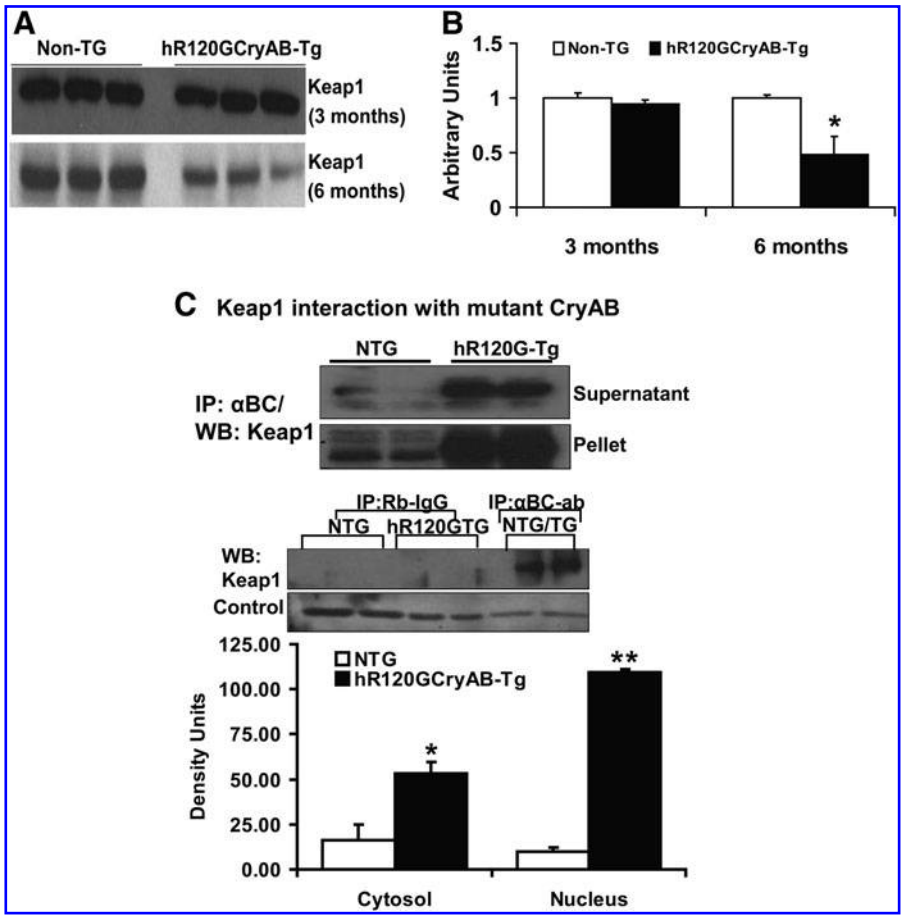

FIG. 8. Determination of Keap1 protein expression and its interactions by IP and WB. (A, B) WB probing Keap1 in the cytosol of NTG and TG hearts: Although there is no significant change in the protein levels of Keap1 among the NTG and TG hearts at 3 months, significant decrease ($p < 0.05$) of cytosolic Keap1 is evident in the TG mouse at 6 months, indicating its sequestration, leading to decreased Nrf2 binding. **(C)** Determination of Keap1 and mutant CryAB protein interactions: IP using anti-CryAB, Keap1 WBs showing robust interactions among these proteins in the TG mouse heart tissue at 6 months, indicating possible sequestration of Keap1 into the protein aggregates. Rb-IgG were used for IP with NTG/TG cytosol. WB images are representative of multiple analysis ($n = 4$ or more) and are statistically significant ($^*p < 0.01$; $^{**}p < 0.05$). Densitometry analysis confirmed significant increase of CryAB and Keap1 aggregation in cytosol and nucleus of TG mice.

mouse hearts at 6 months, suggesting potential sequestration of Keap1 favoring Nrf2 dissociation. Continued synthesis of mutant protein in the TG mouse heart challenges the intracellular environment and activates compensatory pathways, including heat-shock protein (Hsp) signaling (29, 35). Our data suggest that mutant protein stress is also able to activate and upregulate the Nrf2-dependent antioxidant response more substantially than the basal/physiological conditions. Further, our central finding authenticated sustained production and self-oligomerization of dominant negative mutant CryAB sequesters Keap1 (susceptible for conformational changes due to its cysteine rich and redox sensitive nature) and leading to its dysfunction that promotes prolonged dissociation of Nrf2-Keap1 complex; thereby, Nrf2 is freed from ubiquitination, leading to constitutive translocation into the nucleus of TG mouse, which might activate reductive compensation pathways to cause RS. Such chronic activation of master transcription factor Nrf2 resulted in sustained transactivation of ARE-dependent antioxidants in the MPAC contributing to RS. In summary, Keap1-Nrf2 segregation may be plausible contributing mechanism in hR120G CryAB-induced RS and cardiomyopathy (Fig. 9).

Sustained nuclear translocation is necessary and sufficient for contributing to RS in the MPAC

Usually, mutant proteins serve as bona-fide stimulus of stress response pathways to prevent protein aggregation and enhance quality control by degrading unwanted proteins (29, 36). Here we show evidence, besides induction of stress pathways that are involved either in chaperone function or in ubiquitin proteasome system, for the prolonged activation of major antioxidant pathways at transcriptional and translation levels. The importance of Nrf2 in affording protection during oxidative stress has been reported in several studies (18, 19, 24, 33, 37, 48, 50). In association with other proteins, such as small maf proteins, ARE binding protein-1 and other coactivators, Nrf2 binds to ARE, leading to transcriptional induction of target genes (11, 13, 24, 37, 47). Consistent with the nuclear accumulation of Nrf2 and increased binding to ARE in TG mouse hearts (as shown in Figs. 3 and 4), transcription of most of the ARE containing antioxidants was significantly upregulated during MPAC, along with elevated GSH levels, contributing to RS in the TG mouse (29, 30). Profound upregulation of the key antioxidants under the control of Nrf2 activation might be an adaptive mechanism to overcome the mutant protein aggregation expression in TG myopathic hearts.

Conclusion

In this report, we present evidence that sustained Nrf2 activation and its nuclear translocation as one of the causal mechanism for RS in the mouse heart overexpressed with mutant human R120GCryAB transgene. Based on the molecular and biochemical data obtained, we present novel and contributing mechanisms for the RS in this mouse heart failure model that simulates human heart disease.

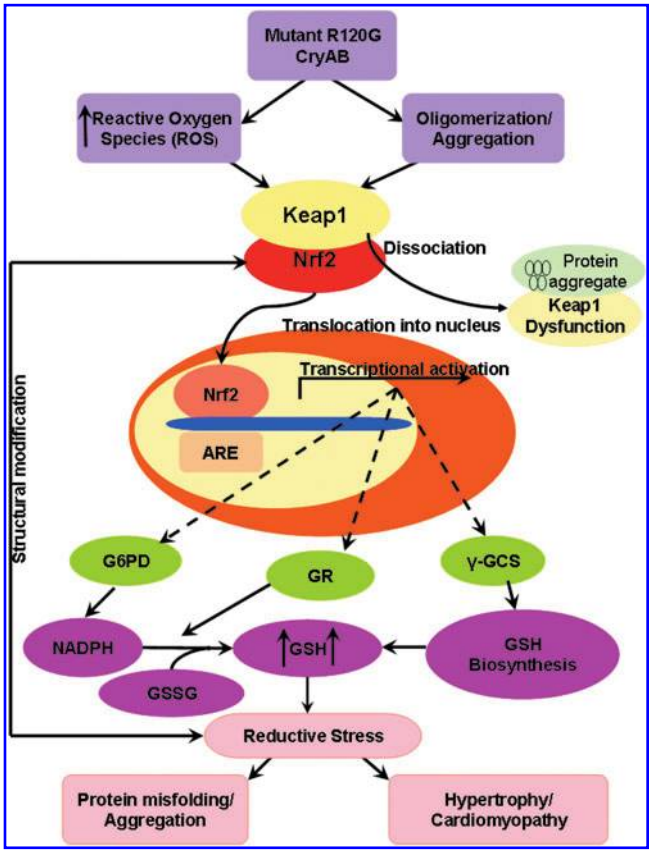

FIG. 9. Schematic proposal for Nrf2 activation and mechanism for reductive stress in the mutant-protein aggregation cardiomyopathy. (For interpretation of the references to color in this figure legend, the reader is referred to the web version of this article at www.liebertonline.com/ars).

Future Directions and Therapeutic Implications

Indeed, our previous findings have claimed that expression of the antioxidant genes early on (before the onset of cardiac hypertrophy) in the TG mouse could be a potential "Bio-Signature" for the prediction/prognosis of RS-dependent cardiomyopathy (30). The current results demonstrate that there is ROS generation and Keap1 sequestration into protein aggregates, which leads to dissociation of Nrf2-Keap1 complex and promotes Nrf2 activation to cause or contribute to RS/PAC. Thus, future experiments should test if abrogating Nrf2 (partial or complete knockdown) could prevent RS/protein aggregation and thereby rescues the TG mouse from cardiac hypertrophy/heart failure.

Acknowledgments

Beginning Grant-In Aid Award from the American Heart Association, Western States Affiliate (0865015F; July 2008–December 2010), and Pilot Grant on Aging (Center for Aging, University of Utah; July 2009–June 2011) to Namakkal Soorappan Rajasekaran, Ph.D., resources from Dr. Ivor Benjamin's laboratory and Dr. Jay L. Zweier's laboratory (NIH grants HL63744, HL65608, and HL38324) provided support for this work. The authors appreciate the helpful suggestions and comments from Dr. John R. Hoidal (Chair of Internal Medicine, University of Utah) and Dr. Dennis Winge (Professor of Medicine). Authors thank Dr. Goutam Karan for his expert help in performing whole-heart images/microscopy. Mrs. Vasanthi Rajasekaran provided extensive technical assistance in performing WBs, scanning and density analysis of images, and preparing graphs. Ms. Jennifer Schroff provided editorial assistance.

Author Disclosure Statement

No competing financial interests exist.

References

1. Cardounel AJ, Xia Y, and Zweier JL. Endogenous methylarginines modulate superoxide as well as nitric oxide generation from neuronal nitric-oxide synthase: differences in the effects of monomethyl- and dimethylarginines in the presence and absence of tetrahydrobiopterin. *J Biol Chem* 280: 7540–7549, 2005.
2. Chen Q, Liu JB, Horak KM, Zheng H, Kumarapeli AR, Li J, Li F, Gerdes AM, Wawrousek EF, and Wang X. Intrasarcoplasmic amyloidosis impairs proteolytic function of proteasomes in cardiomyocytes by compromising substrate uptake. *Circ Res* 97: 1018–1026, 2005.
3. Chen W, Sun Z, Wang XJ, Jiang T, Huang Z, Fang D, and Zhang DD. Direct interaction between Nrf2 and p21(Cip1/WAF1) upregulates the Nrf2-mediated antioxidant response. *Mol Cell* 34: 663–673, 2009.
4. Clements CM, McNally RS, Conti BJ, Mak TW, and Ting JP. DJ-1, a cancer- and Parkinson's disease-associated protein, stabilizes the antioxidant transcriptional master regulator Nrf2. *Proc Natl Acad Sci U S A* 103: 15091–15096, 2006.
5. Delbosc S, Paizanis E, Magous R, Araiz C, Dimo T, Cristol JP, Cros G, and Azay J. Involvement of oxidative stress and NADPH oxidase activation in the development of cardiovascular complications in a model of insulin resistance, the fructose-fed rat. *Atherosclerosis* 179: 43–49, 2005.
6. Dinkova-Kostova AT, Holtzclaw WD, Cole RN, Itoh K, Wakabayashi N, Katoh Y, Yamamoto M, and Talalay P. Direct evidence that sulfhydryl groups of Keap1 are the sensors regulating induction of phase 2 enzymes that protect against carcinogens and oxidants. *Proc Natl Acad Sci U S A* 99: 11908–11913, 2002.
7. Giordano FJ. Oxygen, oxidative stress, hypoxia, and heart failure. *J Clin Invest* 115: 500–508, 2005.
8. Han Z, Varadharaj S, Giedt RJ, Zweier JL, Szeto HH, and Alevriadou BR. Mitochondria-derived reactive oxygen species mediate heme oxygenase-1 expression in sheared endothelial cells. *J Pharmacol Exp Ther* 329: 94–101, 2009.
9. Hayes JD and McMahon M. The double-edged sword of Nrf2: subversion of redox homeostasis during the evolution of cancer. *Mol Cell* 21: 732–734, 2006.
10. Huang X, Atwood CS, Hartshorn MA, Multhaup G, Goldstein LE, Scarpa RC, Cuajungco MP, Gray DN, Lim J, Moir RD, Tanzi RE, and Bush AI. The A beta peptide of Alzheimer's disease directly produces hydrogen peroxide through metal ion reduction. *Biochemistry* 38: 7609–7616, 1999.
11. Ishii T, Itoh K, Takahashi S, Sato H, Yanagawa T, Katoh Y, Bannai S, and Yamamoto M. Transcription factor Nrf2 coordinately regulates a group of oxidative stress-inducible genes in macrophages. *J Biol Chem* 275: 16023–16029, 2000.
12. Itoh K, Chiba T, Takahashi S, Ishii T, Igarashi K, Katoh Y, Oyake T, Hayashi N, Satoh K, Hatayama I, Yamamoto M, and Nabeshima Y. An Nrf2/small Maf heterodimer mediates the induction of phase II detoxifying enzyme genes through antioxidant response elements. *Biochem Biophys Res Commun* 236: 313–322, 1997.

13. Kobayashi M and Yamamoto M. Molecular mechanisms activating the Nrf2-Keap1 pathway of antioxidant gene regulation. *Antioxid Redox signal* 7: 385–394, 2005.
14. Kobayashi M and Yamamoto M. Nrf2-Keap1 regulation of cellular defense mechanisms against electrophiles and reactive oxygen species. *Adv Enzyme Regul* 46: 113–140, 2006.
15. Kohr MJ, Wang H, Wheeler DG, Velayutham M, Zweier JL, and Ziolo MT. Biphasic effect of SIN-1 is reliant upon cardiomyocyte contractile state. *Free Radic Biol Med* 45: 73–80, 2008.
16. Kono Y and Fridovich I. Superoxide radical inhibits catalase. *J Biol Chem* 257: 5751–5754, 1982.
17. Kwak MK, Itoh K, Yamamoto M, and Kensler TW. Enhanced expression of the transcription factor Nrf2 by cancer chemopreventive agents: role of antioxidant response element-like sequences in the nrf2 promoter. *Mol Cell Biol* 22: 2883–2892, 2002.
18. Lee JM, Li J, Johnson DA, Stein TD, Kraft AD, Calkins MJ, Jakel RJ, and Johnson JA. Nrf2, a multi-organ protector? *FASEB J* 19: 1061–1066, 2005.
19. Li J, Ichikawa T, Villacorta L, Janicki JS, Brower GL, Yamamoto M, and Cui T. Nrf2 protects against maladaptive cardiac responses to hemodynamic stress. *Arterioscler Thromb Vasc Biol* 29: 1843–1850, 2009.
20. Liu H, Colavitti R, Rovira, II, and Finkel T. Redox-dependent transcriptional regulation. *Circ Res* 97: 967–974, 2005.
21. Maloyan A, Gulick J, Glabe CG, Kayed R, and Robbins J. Exercise reverses preamyloid oligomer and prolongs survival in alphaB-crystallin-based desmin-related cardiomyopathy. *Proc Natl Acad Sci U S A* 104: 5995–6000, 2007.
22. Maloyan A, Osinska H, Lammerding J, Lee RT, Cingolani OH, Kass DA, Lorenz JN, and Robbins J. Biochemical and mechanical dysfunction in a mouse model of desmin-related myopathy. *Circ Res* 104: 1021–1028, 2009.
23. Maloyan A, Sayegh J, Osinska H, Chua BH, and Robbins J. Manipulation of death pathways in desmin-related cardiomyopathy. *Circ Res* 106: 1524–1532, 2010.
24. Mann GE, Niehueser-Saran J, Watson A, Gao L, Ishii T, de Winter P, and Siow RC. Nrf2/ARE regulated antioxidant gene expression in endothelial and smooth muscle cells in oxidative stress: implications for atherosclerosis and preeclampsia. *Sheng Li Xue Bao* 59: 117–127, 2007.
25. Martensson J, Jain A, Stole E, Frayer W, Auld PA, and Meister A. Inhibition of glutathione synthesis in the newborn rat: a model for endogenously produced oxidative stress. *Proc Natl Acad Sci U S A* 88: 9360–9364, 1991.
26. Meister A. Glutathione deficiency produced by inhibition of its synthesis, and its reversal; applications in research and therapy. *Pharmacol Ther* 51: 155–194, 1991.
27. Motohashi H and Yamamoto M. Nrf2-Keap1 defines a physiologically important stress response mechanism. *Trends Mol Med* 10: 549–557, 2004.
28. Padmanabhan B, Tong KI, Ohta T, Nakamura Y, Scharlock M, Ohtsuji M, Kang MI, Kobayashi A, Yokoyama S, and Yamamoto M. Structural basis for defects of Keap1 activity provoked by its point mutations in lung cancer. *Mol cell* 21: 689–700, 2006.
29. Rajasekaran NS, Connell P, Christians ES, Yan LJ, Taylor RP, Orosz A, Zhang XQ, Stevenson TJ, Peshock RM, Leopold JA, Barry WH, Loscalzo J, Odelberg SJ, and Benjamin IJ. Human alpha B-crystallin mutation causes oxido-reductive stress and protein aggregation cardiomyopathy in mice. *Cell* 130: 427–439, 2007.
30. Rajasekaran NS, Firpo MA, Milash BA, Weiss RB, and Benjamin IJ. Global expression profiling identifies a novel biosignature for protein aggregation R120GCryAB cardiomyopathy in mice. *Physiol Genomics* 35: 165–172, 2008.
31. Rajasekaran NS, Sathyanarayanan S, Devaraj NS, and Devaraj H. Chronic depletion of glutathione (GSH) and minimal modification of LDL *in vivo*: its prevention by glutathione mono ester (GME) therapy. *Biochim Biophys Acta* 1741: 103–112, 2005.
32. Rangasamy T, Cho CY, Thimmulappa RK, Zhen L, Srisuma SS, Kensler TW, Yamamoto M, Petrache I, Tuder RM, and Biswal S. Genetic ablation of Nrf2 enhances susceptibility to cigarette smoke-induced emphysema in mice. *J Clin Invest* 114: 1248–1259, 2004.
33. Rangasamy T, Guo J, Mitzner WA, Roman J, Singh A, Fryer AD, Yamamoto M, Kensler TW, Tuder RM, Georas SN, and Biswal S. Disruption of Nrf2 enhances susceptibility to severe airway inflammation and asthma in mice. *J Exp Med* 202: 47–59, 2005.
34. Rangasamy T, Misra V, Zhen L, Tankersley CG, Tuder RM, and Biswal S. Cigarette smoke-induced emphysema in A/J mice is associated with pulmonary oxidative stress, apoptosis of lung cells, and global alterations in gene expression. *Am J Physiol Lung Cell Mol Physiol* 296: L888–L900, 2009.
35. Sanbe A, Osinska H, Saffitz JE, Glabe CG, Kayed R, Maloyan A, and Robbins J. Desmin-related cardiomyopathy in transgenic mice: a cardiac amyloidosis. *Proc Natl Acad Sci U S A* 101: 10132–10136, 2004.
36. Su H and Wang X. The ubiquitin-proteasome system in cardiac proteinopathy: a quality control perspective. *Cardiovasc Res* 85: 253–262, 2010.
37. Sussan TE, Rangasamy T, Blake DJ, Malhotra D, El-Haddad H, Bedja D, Yates MS, Kombairaju P, Yamamoto M, Liby KT, Sporn MB, Gabrielson KL, Champion HC, Tuder RM, Kensler TW, and Biswal S. Targeting Nrf2 with the triterpenoid CDDO-imidazolide attenuates cigarette smoke-induced emphysema and cardiac dysfunction in mice. *Proc Natl Acad Sci U S A* 106: 250–255, 2009.
38. Tabner BJ, El-Agnaf OM, German MJ, Fullwood NJ, and Allsop D. Protein aggregation, metals and oxidative stress in neurodegenerative diseases. *Biochem Soc Trans* 33: 1082–1086, 2005.
39. Tabner BJ, Turnbull S, Fullwood NJ, German M, and Allsop D. The production of hydrogen peroxide during early-stage protein aggregation: a common pathological mechanism in different neurodegenerative diseases? *Biochem Soc Trans* 33: 548–550, 2005.
40. Takimoto E, Champion HC, Li M, Ren S, Rodriguez ER, Tavazzi B, Lazzarino G, Paolocci N, Gabrielson KL, Wang Y, and Kass DA. Oxidant stress from nitric oxide synthase-3 uncoupling stimulates cardiac pathologic remodeling from chronic pressure load. *J Clin Invest* 115: 1221–1231, 2005.
41. Thimmulappa RK, Lee H, Rangasamy T, Reddy SP, Yamamoto M, Kensler TW, and Biswal S. Nrf2 is a critical regulator of the innate immune response and survival during experimental sepsis. *J Clin Invest* 116: 984–995, 2006.
42. Varadharaj S, Steinhour E, Hunter MG, Watkins T, Baran CP, Magalang U, Kuppusamy P, Zweier JL, Marsh CB, Natarajan V, and Parinandi NL. Vitamin C-induced activation of phospholipase D in lung microvascular endothelial cells: regulation by MAP kinases. *Cell Signal* 18: 1396–1407, 2006.
43. Varadharaj S, Watkins T, Cardounel AJ, Garcia JG, Zweier JL, Kuppusamy P, Natarajan V, and Parinandi NL. Vitamin C-induced loss of redox-dependent viability in lung microvascular endothelial cells. *Antioxid Redox Signal* 7: 287–300, 2005.

44. Venugopal R and Jaiswal AK. Nrf1 and Nrf2 positively and c-Fos and Fra1 negatively regulate the human antioxidant response element-mediated expression of NAD(P)H:quinone oxidoreductase1 gene. *Proc Natl Acad Sci U S A* 93: 14960–14965, 1996.
45. Wakabayashi N, Dinkova-Kostova AT, Holtzclaw WD, Kang MI, Kobayashi A, Yamamoto M, Kensler TW, and Talalay P. Protection against electrophile and oxidant stress by induction of the phase 2 response: fate of cysteines of the Keap1 sensor modified by inducers. *Proc Natl Acad Sci U S A* 101: 2040–2045, 2004.
46. Wang X, Osinska H, Klevitsky R, Gerdes AM, Nieman M, Lorenz J, Hewett T, and Robbins J. Expression of R120G-alphaB-crystallin causes aberrant desmin and alphaB-crystallin aggregation and cardiomyopathy in mice. *Circ Res* 89: 84–91, 2001.
47. Yamamoto T, Suzuki T, Kobayashi A, Wakabayashi J, Maher J, Motohashi H, and Yamamoto M. Physiological significance of reactive cysteine residues of Keap1 in determining Nrf2 activity. *Mol Cell Biol* 28: 2758–2770, 2008.
48. Zakkar M, Van der Heiden K, Luong le A, Chaudhury H, Cuhlmann S, Hamdulay SS, Krams R, Edirisinghe I, Rahman I, Carlsen H, Haskard DO, Mason JC, and Evans PC. Activation of Nrf2 in endothelial cells protects arteries from exhibiting a proinflammatory state. *Arterioscler Thromb Vasc Biol* 29: 1851–1857, 2009.
49. Zhang DD, Lo SC, Cross JV, Templeton DJ, and Hannink M. Keap1 is a redox-regulated substrate adaptor protein for a Cul3-dependent ubiquitin ligase complex. *Mol Cell Biol* 24: 10941–10953, 2004.
50. Zhu H, Jia Z, Misra BR, Zhang L, Cao Z, Yamamoto M, Trush MA, Misra HP, and Li Y. Nuclear factor E2-related factor 2-dependent myocardiac cytoprotection against oxidative and electrophilic stress. *Cardiovasc Toxicol* 8: 71–85, 2008.

Address correspondence to:
Dr. Namakkal Soorappan Rajasekaran
Divisions of Cardiology & Pulmonary
Department of Internal Medicine
University of Utah Health Science Center
RM # 313/313A, Maxwell Wintrobe Building
Salt Lake City, UT 84132

E-mail: raj.soorappan@hsc.utah.edu

Date of first submission to ARS Central, August 17, 2010; date of final revised submission, November 30, 2010; date of acceptance, December 2, 2010.

Abbreviations Used

Ab = antibody
ANOVA = analysis of variance
Arbp1 = acidic ribosomal phosphoprotein
ARE = antioxidant response element
CMH = 1-hydroxy-3-methoxy-carbonyl-2, 2,5,5- tetramethyl pyrrolidine
CryAB = αB-crystallin
DF = defroxamine
DHE = dihydroethidium
EPR = electron paramagnetic resonance
ESR = electron spin resonance
G6pd = glucose 6 phosphate dehydrogenase
GAPDH = glyceraldehyde 3-phosphate dehydrogenase
GCLC = glutamyl cysteine ligase (catalytic)
GCLM = glutamyl cysteine ligase (modulatory)
Gpx1 = glutathione peroxidase-1
GSH = reduced glutathione
Gsr = glutathione reductase
GSSH = oxidized glutathione
H2DCFDA = dihydro difluro diacetate
HEPES = 4-(2-hydroxyethyl)-1-piperazineethanesulfonic acid
Ho1 = hemoxygenase-1
hR120GCryAB = human mutant αB-crystallin
Hsp = heat-shock protein
HSPB2 = heat-shock protein binding factor-2
IP = immunoprecipitation
KCl = potassium chloride
Keap1 = Kelch-like ECH-associated protein-1
$MgCl_2$ = magnesium chloride
MPA = metaphosphoric acid
MPAC = mutant protein aggregation cardiomyopathy
mRNA = messenger RNA
NaCl = sodium chloride
Nqo1 = NADH-quinone oxidase
Nrf2 = nuclear erythroid 2-related factor 2 (NF-E2)
NTG = nontransgenic
ROS = reactive oxygen species
RS = reductive stress
SOD-1 = super oxide dismutase-1
TBST = tris buffered saline-Tween-20
TG = transgenic
WB = Western blot
γ-GCS = γ-glutamyl cysteine synthase

This article has been cited by:

1. Elisabeth S. Christians, Takahiro Ishiwata, Ivor J. Benjamin. 2012. Small heat shock proteins in redox metabolism: Implications for cardiovascular diseases. *The International Journal of Biochemistry & Cell Biology* **44**:10, 1632-1645. [CrossRef]
2. Corey J. Miller, Sellamuthu S. Gounder, Sankaranarayanan Kannan, Karan Goutam, Vasanthi R. Muthusamy, Matthew A. Firpo, J. David Symons, Robert Paine, John R. Hoidal, Namakkal Soorappan Rajasekaran. 2012. Disruption of Nrf2/ARE signaling impairs antioxidant mechanisms and promotes cell degradation pathways in aged skeletal muscle. *Biochimica et Biophysica Acta (BBA) - Molecular Basis of Disease* **1822**:6, 1038-1050. [CrossRef]
3. Houman Ashrafian, Gabor Czibik, Mohamed Bellahcene, Dunja Aksentijevi#, Anthony C. Smith, Sarah J. Mitchell, Michael S. Dodd, Jennifer Kirwan, Jonathan J. Byrne, Christian Ludwig, Henrik Isackson, Arash Yavari, Nicolaj B. Støttrup, Hussain Contractor, Thomas J. Cahill, Natasha Sahgal, Daniel R. Ball, Rune I.D. Birkler, Iain Hargreaves, Daniel A. Tennant, John Land, Craig A. Lygate, Mogens Johannsen, Rajesh K. Kharbanda, Stefan Neubauer, Charles Redwood, Rafael de Cabo, Ismayil Ahmet, Mark Talan, Ulrich L. Günther, Alan J. Robinson, Mark R. Viant, Patrick J. Pollard, Damian J. Tyler, Hugh Watkins. 2012. Fumarate Is Cardioprotective via Activation of the Nrf2 Antioxidant Pathway. *Cell Metabolism* **15**:3, 361-371. [CrossRef]